CARBON letters

Note
Carbon Letters Vol. 21, 86-92 (2017)

Formation of nanojoints between carbon nanotubes and copper nanoparticles

Jagjiwan Mittal and Kwang Lung Lin[♠]

Department of Material Science and Engineering, National Cheng Kung University, Tainan 70101, Taiwan

Article Info

Received 13 February 2016
Accepted 14 October 2016

[♠]**Corresponding Author**
E-mail: matkllin@mail.ncku.edu.tw
Tel: +886-62759602

Open Access

DOI: http://dx.doi.org/10.5714/CL.2017.21.086

This is an Open Access article distributed under the terms of the Creative Commons Attribution Non-Commercial License (http://creativecommons.org/licenses/by-nc/3.0/) which permits unrestricted non-commercial use, distribution, and reproduction in any medium, provided the original work is properly cited.

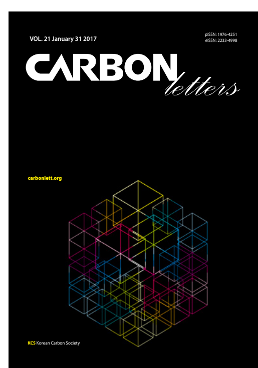

http://carbonlett.org

pISSN: 1976-4251
eISSN: 2233-4998

Copyright © Korean Carbon Society

Exceptional properties and a one dimensional structure make carbon nanotubes (CNTs) a promising candidate for future applications in the electronic industry [1-3]. Because of their smaller dimensions and higher conductivity as compared to copper, multi-walled carbon nanotubes (MWCNT) may increase the bandwidth density of global interconnects [4]. They demonstrate charge carrier mean free paths between 500 nm and 10 µm as compared to 40 nm in metals. CNTs can carry exceptionally high current densities of up to 10^{10} A cm^{-2} even at elevated temperatures [5,6]. CNTs are expected to demonstrate resistance to electromigration higher than that of Cu-based interconnects [7]. However, fabrication difficulties are a major hurdle for developing CNTs as interconnects. The main cause of these difficulties is the difficulty of development of reliable contacts because of the low surface reactivity of CNTs with metals [8]. Sn based alloys have been used to improve the electrical conductivity and interconnections in the soldering field [9]. The electrical resistivity of the polyether sulfone filled with 20% of nickel-coated carbon fiber was reduced by a factor of 2000 by adding 2 vol% tin-lead particles [10]. In one study, Sn coated CNTs were connected on Cu metal [11]. However, Sn coated CNT provides only an outer graphene layer for connecting with Cu. The inner layers remain insulated because the nanotubes are mostly closed. Further, this outer graphene layer can be corrupted because Sn is attached on the outermost graphene layer of the nanotube through the oxygen generated during oxidation. Besides this, the connections can occur anywhere along the length of the surface of the coated nanotube, instead of coating at the terminals of the nanotube, which is useful for circuit purposes. Therefore, there is a need for a method to produce end to end connections. One feasible option is to fill the open CNTs with Sn without coating on the surface.

Metallic nanoparticles such as Cu nanoparticles have received great attention due to their applications in a wide range of electronic devices [12], particularly in flexible electronics [13]. Copper nanoinks have been considered as low-cost nanoinks for printed electronics [14,15]. Cu nanoparticles are also suitable for the production of Multi-Layer Ceramic Condensor (MLCC) internal electrodes and other electronic components in electronic slurries for the miniaturization of microelectronic devices [16]. The high conductivity, flexibility and comparative size with CNTs makes Cu nanoparticles a good potential interconnect material for developing nanocircuits in flexible electronics [17]. However, due to differences in reactivity and structure, joining CNTs with Cu nanoparticles is a big challenge.

The present work developed processes for producing various types of hybrid MWCNTs incorporating Sn. Chemical mechanisms for these processes were proposed. Hybrid MWCNTs were used in the present study to produce nanojoints between two nanomaterials, namely Cu and CNTs, which have dissimilar levels of reactivity.

Commercial Cu nanoparticles with an average size of 20 nm, prepared by electrical explosion method, were used for the present study. The 110–170 nm (outer diameter) MWCNTs were heated in O_2 at 250°C for 30 min to open the closed ends and induce surface oxidation. A portion of the oxidized nanotubes was treated with $NaBH_4$ to reduce the oxidized surface. The oxidized or reduced MWCNTs were then stirred with $SnCl_2$ in HCl, as described elsewhere [18]. The mixing with $SnCl_2$ solution produces hybrid MWCNTs with SnO_2 coating/filling or both. The hybrid MWCNTs and Cu nanoparticles were sprayed on copper grids

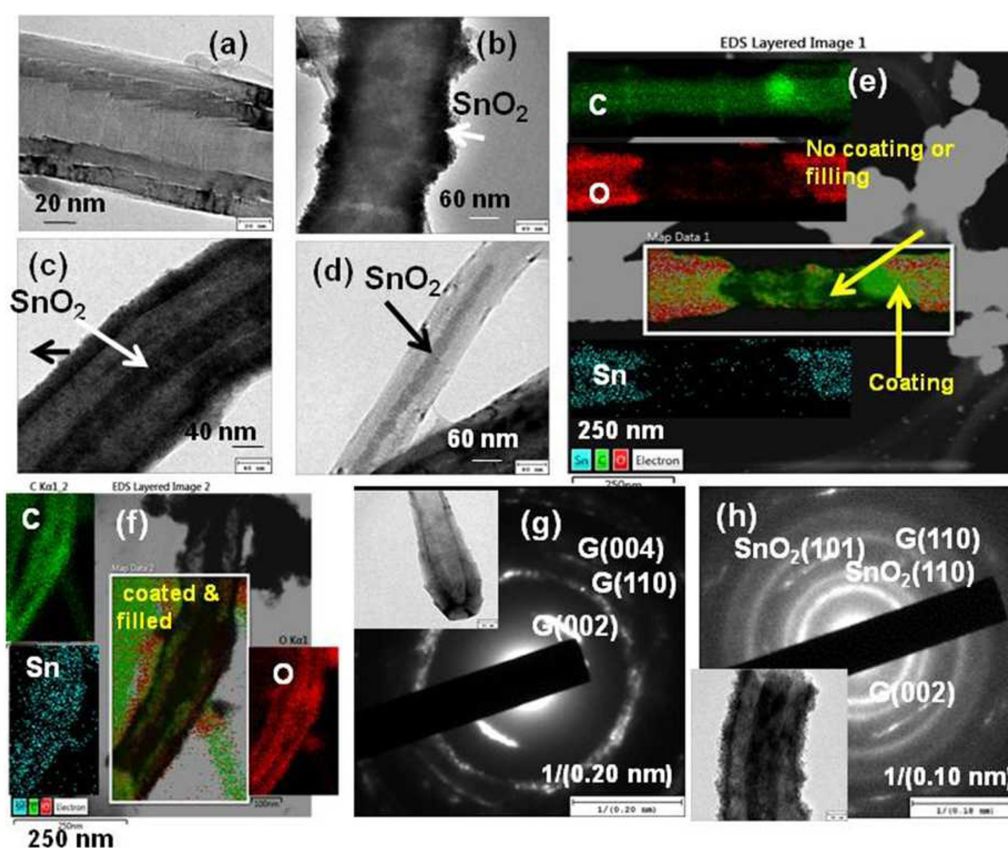

Fig. 1. High resolution transmission electron microscope micrographs show multi-walled carbon nanotubes (MWCNTs) as follows: (a) pristine (b) SnO_2 coated on the surface (c) SnO_2 coated on the surface and filling the inside of the cavity (d) SnO_2 filling the nanotube but not coated on the surface. Energy dispersive X-ray spectroscopy (EDS) mapping demonstrating elemental analysis of (e) uncoated or unfilled, coated shown in frame (f) coated and filled parts of MWCNT shown in frame, and electron diffractions of (g) a pristine MWCNT (h) a coated and filled MWCNT.

having a lacey carbon film. This film provides better visualization of the CNTs at higher magnifications [19]. The grids were heated in a furnace under a 5% H_2/N_2 gas flow at 250°C for 30 min and thereafter cooled to room temperature. The samples were investigated using a JEOL 7001F scanning electron microscope (SEM) and a JEOL 2100 high resolution transmission electron microscope (HRTEM) with 10 keV and 200 keV beam energy having resolutions of 1.5 nm and <0.19 nm, respectively. The HRTEM micrographs were further analyzed using fast Fourier transform (FFT). Elemental analyses of the samples were conducted with energy dispersive X-ray spectroscopy (EDX). The crystal structures were analyzed with electron diffraction (ED).

The HRTEM micrograph in Fig. 1a shows that the MWCNTs have an outer diameter of around 100 nm and an inner diameter of ~40 nm. The pristine nanotube are coated when refluxed with the acidic solution of $SnCl_2$, as shown in Fig. 1b. The outer diameter becomes ~180 nm. The inner tube cavity became invisible under transmission electron microscopy (TEM) due to the thick coating. The coating is uneven, with thickness ranging from 30 to 50 nm. The filling of the cavity is not visible in any of the nanotubes. However, if the pristine nanotubes are heated in air for half an hour prior to $SnCl_2$ solution treatment, the TEM image shows phenomena of surface coating as well as cavity filling (Fig. 1c). It can be observed in the figure that the surface coating and filling inside the nanotube are darker than the graphene layers of the MWCNTs (Fig. 1c and d). The filling material covers the breadth and length of the cavity and seems dense, but some empty spots are also visible. Interestingly, as estimated from the TEM micrographs, the yield of coated nanotubes is >90% in these cases; however, the filling yield is <70%. The reason for this is the different levels of functional groups on the surface and at the opening of nanotubes, which areas are responsible for coating [18] and filling, respectively. It seems that during heating in air, most of the nanotubes were functionalized on the surface, but not all of the nanotubes were opened.

The white inset in Fig. 1e shows a nanotube with thick and thin portions on the sides and in the middle, respectively. The EDX elemental mapping of the HRTEM discloses the presence of Sn, O and C in the thick part where the MWCNTs are coated and/or filled. On the other hand, only C is observed in the thin portion because of the absence of any filling and/or coating. Since the C is from the carbon in the MWCNTs, and oxygen follows the tin both inside and outside of the nanotube, any material present other than MWCNT must be tin oxide. This nanotube is only coated, not filled, as no Sn or O is observed in the cavity; however, another nanotube (shown

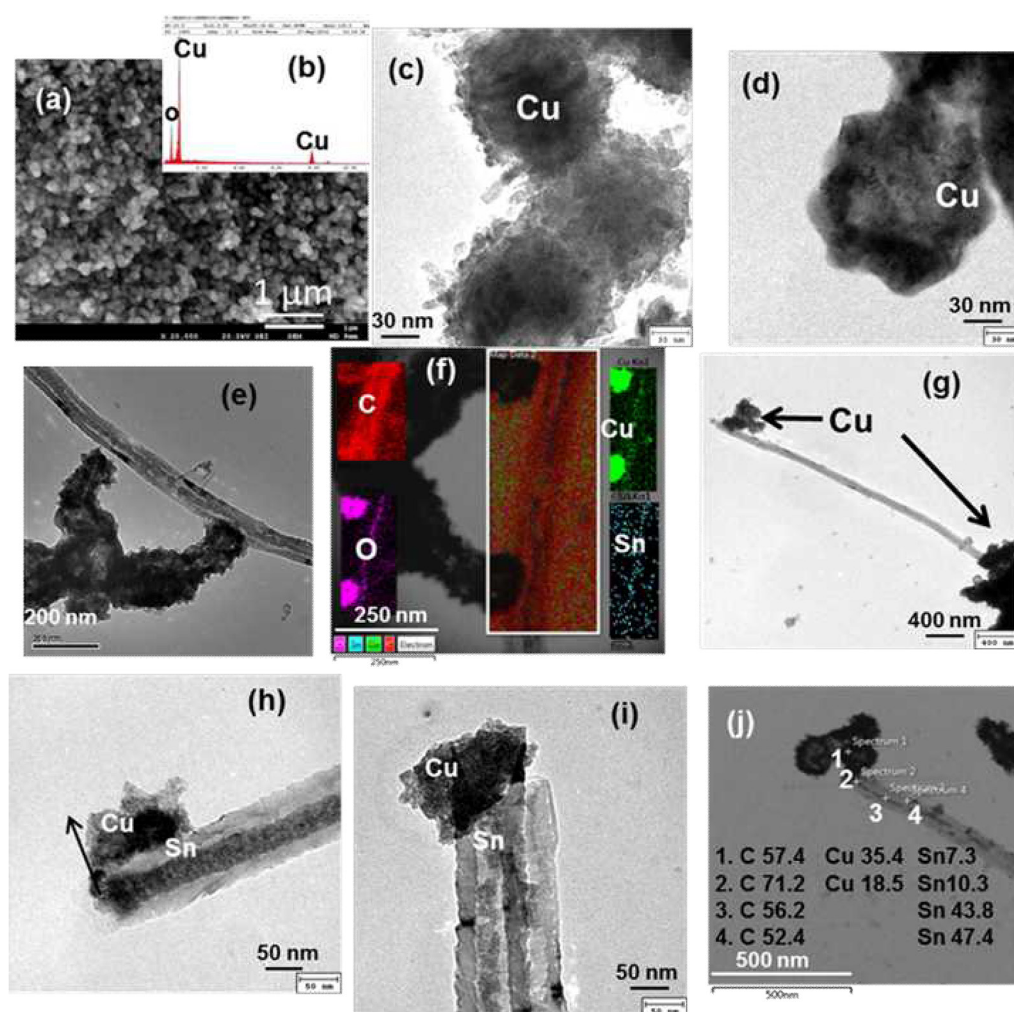

Fig. 2. (a) Field emission scanning electron microscopy micrograph showing Cu nanoparticles (b) point energy dispersive X-ray spectroscopy (EDX) study of Cu nanoparticles high resolution transmission electron microscope (HRTEM) micrographs showing (c) Cu nanoparticles (d) Cu nanoparticles after heating at 250°C (e) formation of interconnects at two places on the surface in the middle of a nanotube with copper nanoparticles (f) EDX mapping study of the portion shown in the frame (g) interconnect of an SnO_2 coated & filled carbon nanotube with Cu nanoparticles at both ends (h, i) HRTEM micrographs showing interconnections at one terminal of the multi-walled carbon nanotubes with Cu nanoparticles (j) point EDX elemental analysis at 1–4 points on the filled nanotube and Cu nanoparticle in the interconnection.

in the white inset) in Fig. 1f reveals the presence of both Sn and O on both the tube surface and the inside of the cavity, which means the nanotubes are both coated and filled with tin oxide. ED, as shown in Fig. 1g and h, reveals that the tin is present in the hybrid nanotubes as SnO_2. As can be observed in Fig. 1g, the three circles in the ED of one pristine CNT belong to the G (002), G (110) and G (004) graphite planes, but there are two planes, (110) and (101), for SnO_2 in addition to the the G (002) and G (110) graphite planes in the filled and coated MWCNT (Fig. 1h).

Fig. 2a provides an SEM micrograph of the Cu nanoparticles. EDX study results in the insert window (Fig. 2b) indicate the presence of Cu and a slight amount of O in the nanoparticles. There is no organic passivation shell on the nanoparticles, as there is no carbon detected in the EDX. The reason for this is that the particles were prepared using electrical the explosion method. Fig. 2c provides HRTEM micrographs of the Cu nanoparticles, which have diameters in the range of 10–15 nm.

The sintering of the Cu nanoparticles takes place when particles are heated to 250°C [20], as shown in Fig. 2d. The HRTEM micrographs in Fig. 2e demonstrate the formation of an interconnect after heating an SnO_2 coated and filled MWCNT and Cu nanoparticles in N_2/H_2 at 250ºC. A single MWCNT is joined with the Cu nanoparticles at two places on the surface of the nanotube. An EDX elemental mapping study of one interconnect, shown in the white inset in Fig. 2f, in which copper nanoparticles are joined with CNT, reveals the presence of Sn, Cu, C and O. Besides nanoparticles, Cu is also observed with the Sn inside the nanotube. This indicates the diffusion of Cu into Sn during the formation of the interconnects. This also discloses the possible formation of some cracks in the nanotube walls during oxidation; from these points, Cu diffuses into the nanotube.

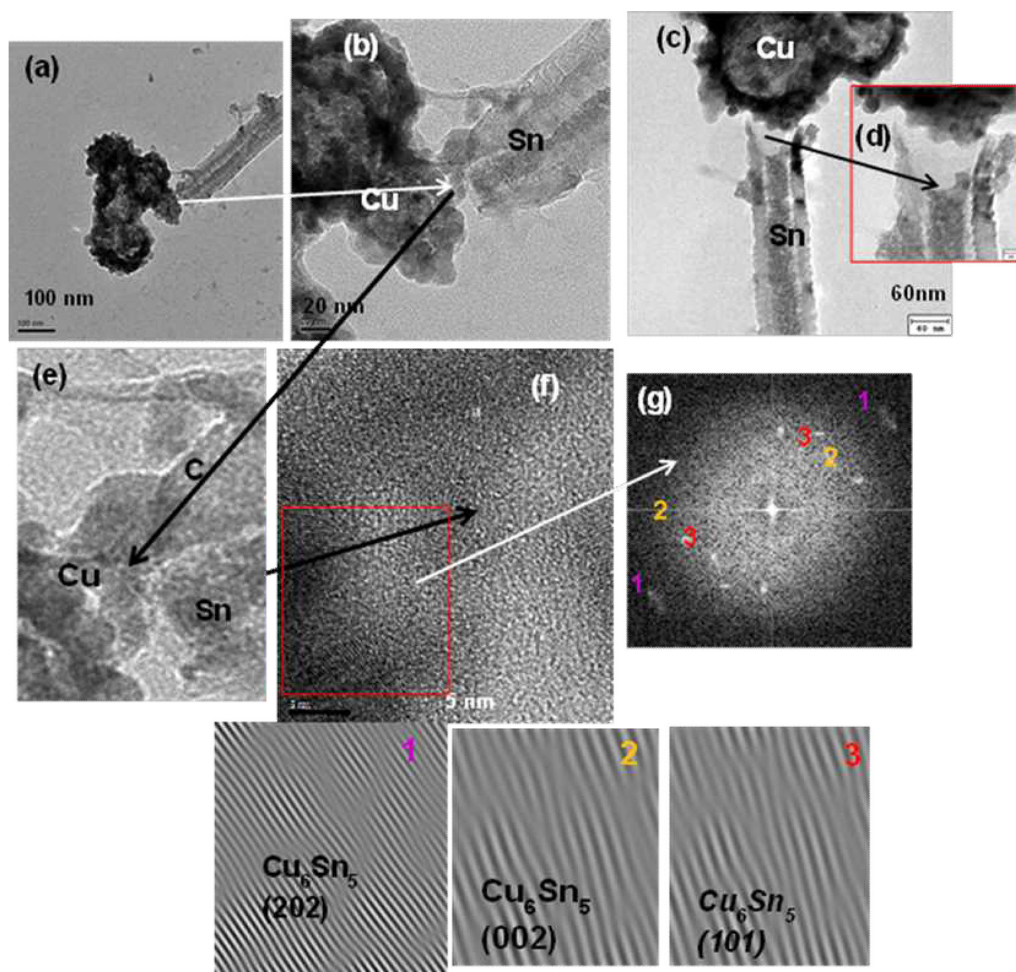

Fig. 3. High resolution transmission electron microscope micrographs showing (a, c) a junction of interconnection between SnO_2 filled and coated nanotubes and Cu nanoparticles (b, d-f) terminals at high magnifications (shown by arrows) (g) fast Fourier transform (FFT) of an area of the micrograph in (f) and inverse FFTs (IFFT) of points 1–3 in FFT of the Cu_6Sn_5 planes.

When a hybrid nanotube filled with SnO_2 inside the cavity without coating on the surface is used to make the interconnections, it can only join with Cu nanoparticles at the open ends of the nanotube. Fig. 2g displays one such connection, where Cu nanoparticles are attached at both terminals of a nanotube. Higher magnifications of the region of attachment of a nanoparticle to a terminal of a filled nanotube are further shown in Fig. 2h and i. Point EDX elemental analysis at points 1 and 2 in Fig. 2j, at the junction between CNT and the Cu nanoparticle shows the presence of C, Sn and Cu, whereas only C and Sn are observed at points 3 and 4, far from the terminal. The atomic percentage of the copper is highest at point 1 and no copper is observed at points 3 and 4. On the other hand, the percentage of Sn increases with the increase in the distance from the copper nanoparticles.

The HRTEM micrographs in Fig.3a and c show the presence of copper nanoparticles at the terminal of the filled CNTs. The magnified views in Fig. 3b and d (inset in Fig. 3c) show the attachment of Cu nanoparticles at the openings of the nanotubes. Since no bonding is possible between Cu and carbon at this temperature, attachment has to take place between Sn inside the nanotubes (or present on the nanotubes in a slight amount) and Cu. Further magnifications of Fig. 3b shown in Fig. 3e and f display the link between the filled MWCNT and the copper nanoparticles through the filled Sn inside the nanotube and the coated Sn at the terminals of the nanotubes.

The ED analysis data shown in Fig. 3g, of the joint area of Fig. 3f, show the existence of amorphous and crystalline structures of the joint. Inverse FFT (IFFT) analysis of the selected area diffraction of patterns 1, 2, and 3 in Fig. 3g are shown at the bottom of Fig. 3. The formation of an amorphous structure along with nano-size crystal planes during soldering with Sn-based solders on the Cu substrate has been shown in earlier studies [21]. The amorphous region is believed to be a result of the interdiffusion between Cu and Sn [21-23]. The IFFT of each plane reveals the formation of Cu_6Sn_5 by (202), (101), (002) crystal planes [24]. The crystal planes show that dislocations exist in the area of analysis. This shows that the appropriate metallization of MWCNT with Sn allows the manufacture of a nanojoint between a CNT and Cu nanoparticles. Joints between Cu nanoparticles and CNT are formed through the formation of Cu_6Sn_5 intermetallics. The joining

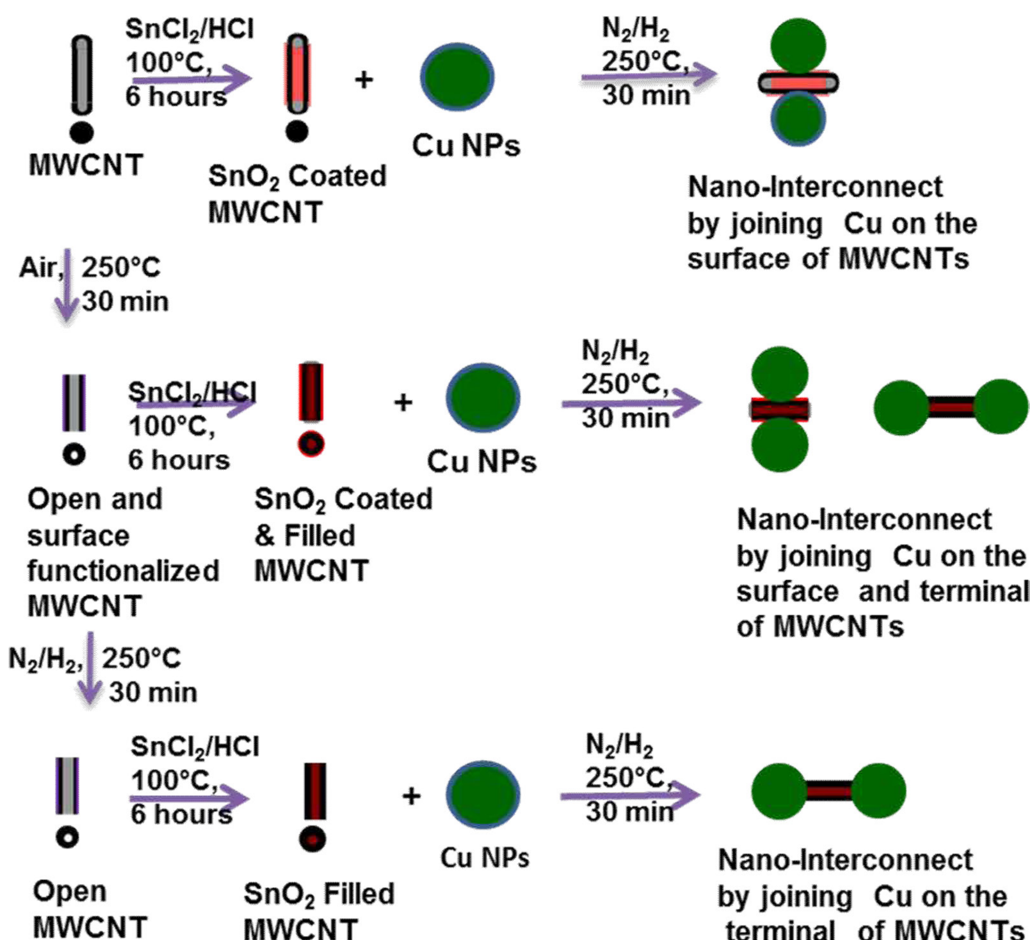

Fig. 4. Sketch illustrating the process for (a) coating of SnO_2 on multi-walled carbon nanotubes (MWCNTs) (B) formation of interconnect by joining Cu on the surface of hybrid MWCNTs (C) oxidation and opening of MWCNTs (D) coating and filling of MWCNTs with SnO_2 (E) formation of nano-interconnects between Cu nanoparticles and hybrid MWCNTs on the surface and at the terminal (F) reduction of oxidized MWCNT (G) SnO_2 filling the inside of the MWCNT (H) formation of interconnect with Cu at the terminal of the SnO_2-filled MWCNTs. NPs, metallic nanoparticles.

can form connections on the surface of the nanotubes or from end to end. This is different from the findings of earlier studies, in which connections either involved using bulk nanotubes or occurred on the surface of nanotubes [11,25-28].

Fig. 4 depicts the mechanism for the coating and filling of the nanotubes and the formation of the interconnections on the copper nanoparticles. If pristine nanotubes are treated with $SnCl_2$, then only the surface is coated with SnO_2 (process A, Fig.4). When these coated nanotubes are heated with Cu nanoparticles in the presence of H_2/N_2, SnO_2 will be reduced to Sn, which reacts with Cu and forms an intermetallic compound, Cu_6Sn_5, on the surface of the nanotubes (reactions 1 & 2). This results in the formation of interconnects at the surface of the nanotubes (process F, Fig. 4).

$$SnO_2 \xrightarrow{H_2/N_2,\ 250°C} Sn \quad (1)$$

$$6Cu + 5Sn \xrightarrow{250°C} Cu_6Sn_5 \quad (2)$$

, when the pristine nanotubes are heated in air (process B, Fig. 4), the O_2 in the air oxidizes the surface of the MWCNTs and opens the CNTs [29]. Refluxing these nanotubes with $SnCl_2$/HCl solution (process C, Fig. 4) not only forms SnO_2 coating on the surface but also fills the inside of the tube with SnO_2. The coating on the surface is due to the formation of bonding between Sn and the oxygenated groups on the surface [18]. On the other hand, filling occurs in open nanotubes due to capillary forces. Reacting these nanotubes with Cu nanoparticles in N_2/H_2 atmosphere (process G, Fig. 4) results in the formation of nanojoints both on the surface and at the ends of the nanotube.

If air-treated nanotubes are heated in N_2/H_2 (process D, Fig. 4), then the oxygen-containing functional groups on the surface are reduced by the H_2, but the nanotubes remain open. Therefore, these nanotubes are filled with SnO_2 during refluxing with $SnCl_2$ (process E, Fig. 4) but are not coated on the surface. Heating joins nanotubes with Cu nanoparticles (process H, Fig. 4) and forms nanojoints at the two terminals of the nanotubes. Since these nanotubes do not have any coating on the surface, the only place where an intermetallic compound can form is at the terminal of the nanotubes.

This study demonstrates the formation of nanojoints between two dissimilar nanomaterials, i.e. CNTs and Cu nanoparticles,

DOI: http://dx.doi.org/10.5714/CL.2017.21.086

using Sn. The hybrid CNTs can be produced by appropriately designing the oxidation, reduction, and refluxing steps to produce coating or filling, or coating/filling with Sn. Connections on the surface or at the terminals of the hybrid CNTs with Cu nanoparticles can be made possible. The joint was formed through the formation of Cu_6Sn_5 intermetallics between Sn and the Cu nanoparticles. The process developed in this study provides a method for developing a CNT-based nanocircuit, which may initiate the development of nanomaterial-based interconnects in microelectronics packaging.

Conflict of Interest

No potential conflict of interest relevant to this article was reported.

Acknowledgements

Support of this study by the National Science Council (NSC) of the Republic of China (Taiwan) under Grant NSC101-2221-E006-117-MY3 is gratefully acknowledged. One of the authors (J. Mittal) is grateful to the NSC for its financial support during the course of this work under Grant NSC102-2811--E-006-048.

References

[1] Berber S, Kwon YK, Tománek D. Unusually high thermal conductivity of carbon nanotubes. Phys Rev Lett, **84**, 4613 (2000). https://doi.org/10.1103/physrevlett.84.4613.

[2] Sun Y, Zhu L, Jiang H, Lu J, Wang W, Wong CP. A paradigm of carbon nanotube interconnects in microelectronic packaging. J Electron Mater, **37**, 1691 (2008). https://doi.org/10.1007/s11664-008-0533-1.

[3] Collins PG, Arnold MS, Avouris P. Engineering carbon nanotubes and nanotube circuits using electrical breakdown. Science, **292**, 706 (2001). https://doi.org/10.1126/science.1058782.

[4] Naeemi A, Meindl JD. Performance Modeling for Carbon Nanotube Interconnects. In: Javey A, Kong J, eds. Carbon Nanotube Electronics, Springer, Boston, 181 (2009).

[5] Wei BQ, Vajtai R, Ajayan PM. Reliability and current carrying capacity of carbon nanotubes. Appl Phys Lett, **79**, 1172 (2001). https://doi.org/10.1063/1.1396632.

[6] de Pablo PJ, Graugnard E, Walsh B, Andres RP, Datta S, Reifenberger R. A simple, reliable technique for making electrical contact to multiwalled carbon nanotubes. Appl Phys Lett, **74**, 323 (1999). https://doi.org/10.1063/1.123011.

[7] Srivastava N, Banerjee KA. A comparative scaling analysis of metallic and carbon nanotube interconnections for nanometer scale VLSI technologies. Proceedings of the 21st international VLSI Multilevel Interconnect Conference (VMIC), Waikoloa, HI, 393 (2004).

[8] Avouris P, Chen Z, Perebeinos V. Carbon-based electronics. Nat Nanotechnol, **2**, 605 (2007). https://doi.org/10.1038/nnano.2007.300.

[9] Kang SK, Sarkhel AK. Lead (Pb)-free solders for electronic packaging. J Electron Mater, **23**, 701 (1994). https://doi.org/10.1007/bf02651362.

[10] Li L, Yih P, Chung DDL. Effect of the second filler which melted during composite fabrication on the electrical properties of short fiber polymer-matrix composites J Electron Mater, **21**, 1065 (1992). https://doi.org/10.1007/bf02665885.

[11] Mittal J, Lin KL. The formation of electric circuits with carbon nanotubes and copper using tin solder. Carbon, **49**, 4385 (2011). https://doi.org/10.1016/j.carbon.2011.06.029.

[12] Hu A, Guo JY, Alarifi H, Patane G, Zhou Y, Compagnini G, Xu CX. Low temperature sintering of Ag nanoparticles for flexible electronics packaging. Appl Phys Lett, **97**, 153117 (2010). https://doi.org/10.1063/1.3502604.

[13] Klauk H, D'Andrade B, Jackson TN. All-organic integrated emissive pixels. Proceedings of the 57th Annual Device Research Conference Digest, Santa Barbara, CA, 162 (1999). https://doi.org/10.1109/drc.1999.806356.

[14] Kim HS, Dhage SR, Shim DE, Hahn H. Intense pulsed light sintering of copper nanoink for printed electronics. Appl Phys A, **97**, 791 (2009). https://doi.org/10.1007/s00339-009-5360-6.

[15] Magdassi S, Grouchko M, Kamyshny A. Copper nanoparticles for printed electronics: routes towards achieving oxidation stability. Materials, **3**, 4626 (2010). https://doi.org/10.3390/ma3094626.

[16] Kang JS, Kim HS, Ryn J, Hahn T, Jang S, Joung JW. Inkjet printed electronics using copper nanoparticle ink. J Mater Sci Mater Electron, **21**, 1213 (2010). https://doi.org/10.1007/s10854-009-0049-3.

[17] Jeong S, Woo K, Kim D, Lim S, Kim JS, Shin H, Xia Y, Moon J. Controlling the thickness of the surface oxide layer on Cu nanoparticles for the fabrication of conductive structures by ink-jet printing. Adv Funct Mater, **18**, 679 (2008). https://doi.org/10.1002/adfm.200700902.

[18] Mittal J, Lin KL. Connecting carbon nanotubes using Sn. J Nanosci Nanotechnol, **13**, 5590 (2013). https://doi.org/10.1166/jnn.2013.7560.

[19] Harris PJF. Carbon nanotubes and other graphitic structures as contaminants on evaporated carbon films. J Microsc, **186**, 88 (1997). https://doi.org/10.1046/j.1365-2818.1997.1930754.x.

[20] Mittal J, Lin KL. Exothermic low temperature sintering of Cu nanoparticles. Mater Charact, **109**, 19 (2015). https://doi.org/10.1016/j.matchar.2015.09.009.

[21] Pan CC, Lin KL. The interfacial amorphous double layer and the homogeneous nucleation in reflow of a Sn-Zn solder on Cu substrate. J Appl Phys, **109**, 103513 (2011). https://doi.org/10.1063/1.3592182.

[22] Lin YW, Lin KL. The early stage dissolution of Ni and the nucleation of Ni-Sn intermetallic compound at the interface during the soldering of Sn-3.5Ag on a Ni substrate. J Appl Phys, **108**, 063536 (2010). https://doi.org/10.1063/1.3484493.

[23] Lin YW, Lin KL. Nucleation behaviors of the intermetallic compounds at the initial interfacial reaction between the liquid Sn3.0Ag0.5Cu solder and Ni substrate during reflow. Intermetallics, **32**, 6 (2013). https://doi.org/10.1016/j.intermet.2012.07.035.

[24] Hwang CW, Kim KS, Suganuma K. Interface in lead-free soldering. J Electron Mater, **32**, 1249 (2003). https://doi.org/10.1007/s11664-003-0019-0.

[25] Nai SML, Wei J, Gupta M. Effect of carbon nanotubes on the shear strength and electrical resistivity of a lead-free solder. J Electron Mater, **37**, 515 (2008). https://doi.org/10.1007/s11664-008-0379-6.

[26] Hayamizu Y, Yamada T, Mizuno K, Davis RC, Futaba DN, Yamura

M, Hita K. Integrated three-dimensional microelectromechanical devices from processable carbon nanotube wafers. Nat Nanotechnol, **3**, 289 (2008). https://doi.org/10.1038/nnano.2008.98.

[27] Zhang Y, Ichihashi T, Landree E, Nihey F, Iijima S. Heterostructures of single-walled carbon nanotubes and carbide nanorods. Science, **285**, 1719 (1999). https://doi.org/10.1126/science.285.5434.1719.

[28] Nihei M, Kondo D, Kawabata A, Sato S, Shioya H, Sakaue M, Iwai T, Ohfuti M, Awano Y. Low-resistance multi-walled carbon nanotube vias with parallel channel conduction of inner shells [IC interconnect applications]. Proceedings of the IEEE 2005 International Interconnect Technology Conference, Burlingame, CA, 234 (2005). https://doi.org/10.1109/iitc.2005.1499995.

[29] Ajayan PM, Ebbesen TW, Ichihashi T, Iijima S, Tanigaki K, Hiura H. Opening carbon nanotubes with oxygen and implications for filling. Nature, **362**, 522 (1993). https://doi.org/10.1038/362522a0.